ACAM - a new imager / spectrograph for the William Herschel Telescope

Chris Benn[a], Kevin Dee[b], Tibor Agócs[a],

[a]Isaac Newton Group, Apartado 321, 38700 Santa Cruz de La Palma, Spain
[b]Engineering & Project Solutions Ltd, Daresbury Science Park, Warrington, WA4 4FS, United Kingdom

ABSTRACT

ACAM will be mounted permanently at a folded-Cassegrain focus of the WHT. It can be used for broad-band or narrow-band optical imaging of an 8.3-arcmin field, or for low-resolution ($R \sim 500$) spectroscopy. As the only wide-field optical imager at the Cassegrain focus, ACAM is designed to cater for a broad range of science programmes, including those requiring rapid response (e.g. gamma-ray bursts, supernovae) or scheduling at awkward intervals (e.g. successive exoplanet transits), and those requiring the use of many filters (e.g. H_α mapping of low-redshift galaxies). The imaging requirements alone are demanding, requiring a trade-off between field of view ($>$ 8 arcmin), PSF ($<<$ seeing), wavelength coverage (UV to near-IR), throughput ($>$ 0.8) and radius-dependent wavelength shift ($<$ 0.5 nm, for narrow-band filters). We discuss how the trade-off was effected and present the final optical and mechanical design, and the expected performance.

Keywords: Wide-field imaging, narrow-band imaging, spectroscopy, VPH gratings, optical design, WHT, ACAM

1. INTRODUCTION

At the 4.2-m William Herschel Telescope (WHT) on La Palma, observers can switch quickly between instruments mounted at Cassegrain, folded-Cassegrain and Nasmyth foci, which allows for considerable flexibility when observing. In particular, a simple imager mounted permanently at the folded Cassegrain focus (the auxiliary-port camera) is much used for rapid-response follow-up of gamma-ray bursts or supernovae (SNe), and for opportunistic imaging of objects being observed with other instruments. Scientific highlights from this camera include the first detection of gravitational microlensing in the quadruply-imaged Einstein-cross quasar[1], identification of the companion star to Tycho Brahe's 1572 supernova[2] and the first detection of the progenitor star of a normal type IIP supernova.[3]

The current imager includes no optics, and offers a field of view only 1.8 arcmin across, which is small compared to the $\approx$ 15-arcmin unvigenetted field of view at the telescope's Cassegrain focus. In addition, the filters installed in the wheel cannot be changed without removing the CCD cryostat. A decision was therefore taken to replace this camera by a re-imager (ACAM) offering a larger field of view, simpler filter changes, and the option of low-resolution spectroscopy.

In Section 2 we summarise the science requirements and other constraints on the design. In Sections 3 – 6, we describe the optical design, the detector, the mechanical design and the instrument-control software.

2. SCIENCE REQUIREMENTS, DESIGN CONSTRAINTS

The science requirements were drawn up by: (1) reviewing the science for which the camera is currently used, and considering how the observational results could be improved; and (2) considering what new science could be carried out, given realistic options for extending the field of view, wavelength coverage, spectroscopic resolution etc.

This led to a set of science programmes which we felt were likely to have high future scientific impact:
• Rapid follow-up imaging of GRBs and SNe. A wide field is important to allow accurate photometry relative

E-mail: crb@ing.iac.es

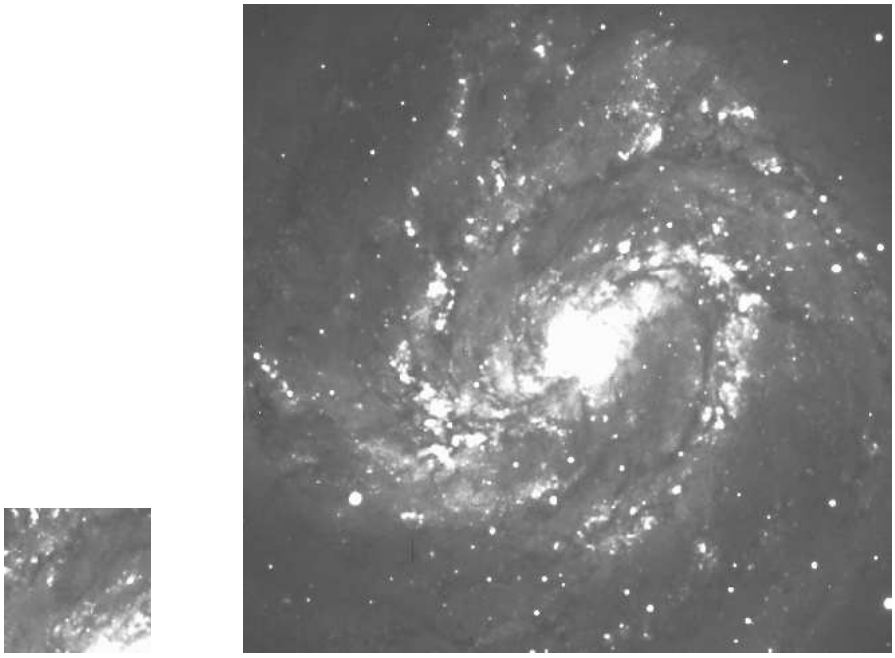

Figure 1. M81, as it would be imaged by cameras with fields 1.8 and 8 arcmin across, representing the current auxiliary-port camera and ACAM respectively.

to other stars of similar brightness. Low-resolution spectroscopy (UV to near-IR) is desirable, for determining e.g. SN type, or approximate redshift.

• Observations of the light curves of exoplanets transiting their host stars. Such transits typically occur every few days and last a few hours, so observations of these need to share the nights with science programmes using other instruments. The transits may be only a few mmag deep, so a wide field is again required, for high-precision relative photometry.

• Wide-field broad-band imaging, catering for the kind of science currently carried out using the WHT's prime-focus camera (16-arcmin field), but without the need for a labour-intensive top-end change.

• Wide-field narrow-band imaging, e.g. to map star-formation in low-redshift galaxies, using filters provided by visitors, or from ING's existing comprehensive collection of narrow-band filters,

• High-throughput, low-resolution spectroscopy of very faint objects e.g. candidate high-redshift galaxies or quasars.

• Near-simultaneous optical/IR imaging and spectroscopy, when the WHT's main near-IR instrument, LIRIS, is mounted at the straight-through Cassegrain focus.

From the above, we derived a set of science requirements for broad-band imaging, including:

(1) Field of view as large as reasonably possible, up to a maximum diameter of 15 arcmin, outside which the field is vignetted by the Cassegrain acquisition and guiding (A&G) unit.

(2) Wavelength range, ideally, from the atmospheric cutoff ($\approx$ 330 nm) to the reddest wavelengths detectable by CCDs ($\approx$ 1000 nm).

(3) Point-spread-function (PSF) small enough that the best La Palma seeing (0.5 arcsec) is not significantly degraded. In particular, the performance should over the central 1.8-arcmin field should be as good as that offered by the current auxiliary-port camera. The PSF requirement also forces a pixel scale $<\sim$ 0.25 arcsec pixel^{-1}, for adequate sampling of the seeing.

(4) Throughput of optics (excluding telescope mirrors) $>\sim$ 0.8, so that any loss of performance relative to the current camera (no optics, but poorer CCD QE) is small.

(5) Differential optical distortion of the field $<\sim$ 1 arcsec between 330 and 1000 nm, at the edge of the field, to simplify multi-band observations of extended objects.

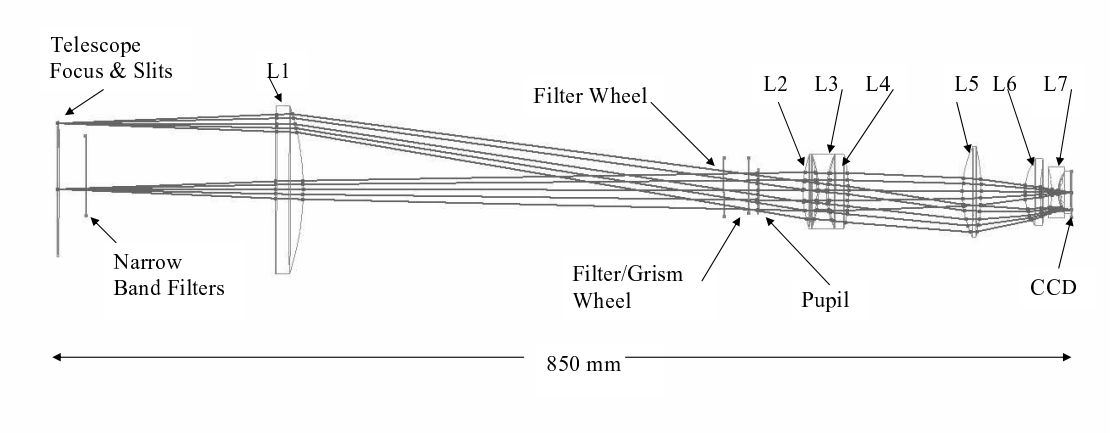

Figure 2. Optical layout of ACAM. The f/11 folded-Cassefrain focus (left) lies 650 mm from the 45^o flat (not shown) at the centre of the Cassegrain A&G box, and is just outside the wall of that box. Lens 1 is the (post-focus) field lens. Lenses 2 to 7 provide the re-imaging. Lens 7 is actually the cryostat window, a few mm from the CCD. The distance from telescope focus to CCD is $\approx$ 850 mm. The pupil (defined as the plane where the bundle of rays from all positions in the field has minimum footprint) lies 35 mm before lens 2. For robustness, and ease of alignment, lenses 2 to 6 are mounted in one lens barrel. The two wheels for the filters and dispersing elements are therefore positioned just before lens 2 (rather than between lenses 4 and 5). The spectroscopic slits are mounted on a moveable slide in the focal plane, before the field lens. The same slide includes two extra mounts for narrow-band filters.

(6) Flexure < (spatial resolution / 2) during an exposure, i.e. < 1 pixel over 30 mins.
(7) Pupil diameter < 50 mm, to allow the use of small filters in the near-pupil space.

For narrow-band imaging, there are two additional requirements:
(8) The change in the effective central wavelength of a narrow-band filter, as a function of radius in the field of view, must be much less than the bandpass of the filter (which can be as small as 1.5 nm), otherwise e.g. an emission-line image of an extended object will be vignetted.
(9) Straightforward installation of filters, since a given narrow-band observing programme may use many different filters (to match the galaxy redshifts).

The additional requirements for spectroscopy are:
(10) Spectroscopic resolution of at least a few hundred, when using a slit of width 1 arcsec, on-axis. Most of the scientific impact is likely to come from observing $\approx$ seeing-sized objects, so good spectroscopic resolution is less important off-axis.
(11) A choice of slits, to match different seeing conditions, and of dispersers, to allow different trade-offs between spectroscopic resolution, wavelength range and throughput.
(12) A means of carrying out target acquisition.
(13) A means of carrying out wavelength calibration.

There are in addition a number of mechanical constraints, e.g. on total length, to ensure that the end of the instrument will not collide with the telescope fork.

3. OPTICAL DESIGN

The main goal of the optical design is to satisfy the imaging requirements. Spectroscopy is then to be incorporated if it does not compromise the imaging performance.

3.1. Imaging

The starting point for the design of ACAM was an optical train comprising a field lens, a collimating lens (to create the pupil) and camera lenses (making 5 lenses in all) to provide the field reduction. The field lens makes

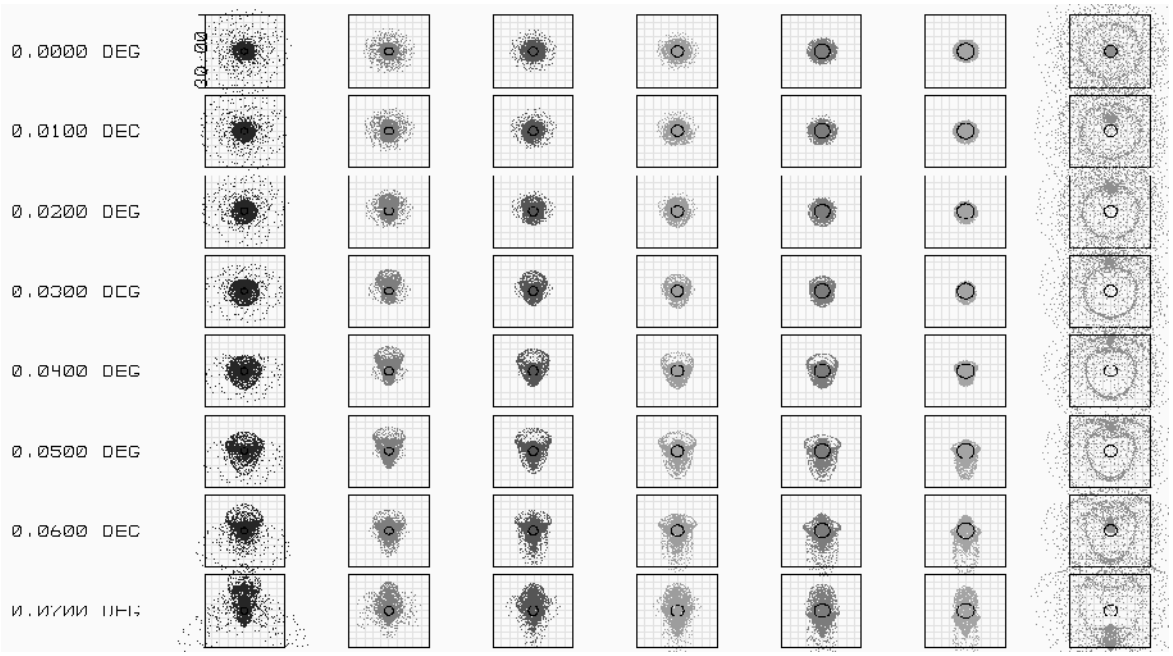

Figure 3. Predicted image quality for the final optical design, as a function of wavelength (360, 450, 550, 650, 820, 885 nm, left to right) and radius in the field of view (0 to 4.2 arcmin, top to bottom). The box sizes are 0.5 arcsec, corresponding to 2 pixels on the CCD (30 microns). Columns 1 to 6 show the spot diagrams after refocus of the telescope. Column 7 shows the 6 spot diagrams superimposed, without refocus, which gives an idea of the optical quality for spectroscopy. At all wavelengths, and at all radii in the focal plane out to 4.2 arcmin, the predicted PSFs are small enough that the natural seeing (> 0.5 arcsec) will not significantly be degraded. The black circles indicate the size of the Airy disk.

the system more compact, and reduces the need for a strong collimator. It is located post-focus, rather than pre-focus, because of the proximity of the focal plane to the wall of the Cassegrain A&G box.

Initial modelling with ZEMAX showed that it is not possible to build a re-imager for the f/11 Cassegrain focus which delivers good PSF at all radii in a 16-arcmin field, at all wavelengths from UV to near-IR, without incorporating many optical surfaces, which would then compromise the throughput. Providing a good PSF in the UV and/or at large radii is especially demanding of the optics. We therefore decided to optimise the modelling for a field of view 8.3 arcmin across (20 x the area of the current camera, Fig. 1), corresponding to 2000 pixels (a convenient detector size) at 0.25 arcsec pixel^{-1}.

Further ZEMAX modelling showed that (1) the imaging performance requirements could not be met with 5 lenses, and (2) having a flat cryostat window (for easy interchangeability with other CCDs) is a major constraint on the rest of the optical design.

We therefore optimised two 6-lens designs. Each comprised a field lens and 5 camera lenses, the last of which is a field-flattener (negative lens). One design included a separate flat cryostat window, while in the other design the final lens (the field-flattener) became the cryostat window. In the latter, the field-flattening lens is closer to the CCD and ZEMAX showed that this not only improves the image quality attainable, but considerably relaxes the tolerances on the other lenses.

This persuaded us to set aside our operational preference for a flat cryostat window. The design with the active cryostat window was then further optimised to improve the throughput. Possible high-throughput substitute glasses were identified for each lens, and ZEMAX then iterated on these using the 'Hammer' global optimisation algorithm. This allows ZEMAX to optimise simultaneously the radius, thickness and material of each lens, ensuring that only real glasses are used (as opposed to finding a solution requiring a material with unattainable properties). The material of lens 7 was excluded from optimisation; to eliminate background radiation, it must

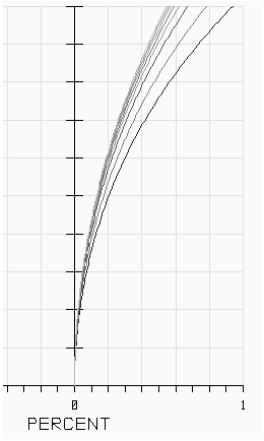

Figure 4. Predicted field distortion as function of radius in the field (vertical axis, extending to 4.2 arcmin) and wavelength (the curves represent wavelengths from 1000 to 340 nm, left to right). The maximum relative distortion between wavelengths 340 and 1000 nm is 0.4% at the field edge, corresponding to $\approx$ 1.0 arcsec.

be fused silica. At this point, we also added one extra lens, to improve image quality and reduce distortion, bringing the total number of lenses to 7: a field lens, and 6 camera lenses, the last of which is the cryostat window (Fig. 2).

The resulting design then satisfied the basic broad-band imaging requirements, with regard to image quality as a function of radius in the field and wavelength, even in the UV (Fig. 3).

As part of the optimisation process, the sensitivity of the design to manufacturing and assembly tolerances was also minimised, by including them explicitly in the calculation of the merit function. The end product is a cheaper and more stable design which is ready for manufacture. Improved tolerances come at the expense of slightly degraded PSF and throughput, but the science requirements are still met. A detailed analysis of the effects of temperature changes was also carried out. It showed that these effects could be compensated for by refocusing the telescope.

Finally, to minimise the cost, the design was matched to existing test plates and tools (for manufacturing lenses of given physical size) and the design was re-optimised.

Prior to manufacture, the melt data for the lens blanks will be obtained, and the design re-optimised. After manufacturing, the actual thickness of each lens will be obtained, and the air spaces will again be re-optimised. Finally a double pass test of the on-axis image at 633 nm will be carried out to check image quality. Interferometry from this measurement will be used to check for possible errors in assembly.

The final design uses several materials for the lenses: Lens 1 is of N-BAK2; 2 and 4 are CaF_2, 3 is N-BAK1, 5 is S-FPL53, 6 is S-LAL7 and 7 is fused silica. The diameter of the field lens (lens 1) is 140 mm. The diameters of lenses 2 - 7 range 40 - 80 mm.

The net throughput of the 7 lenses, with anti-reflection coating, is $\approx$ 0.80. The loss of throughput relative to the current (optics-free) auxiliary-port camera is approximately compensated for by the improved efficiency of the CCD (peak QE = 0.9). In imaging mode, the total throughput of the telescope, Cassegrain fold flat, instrument and CCD will be $\approx$ 0.49.

Mild distortion is not a problem for imaging in one band. For multi-band imaging (e.g. of galaxies subtending several arcmin), it may be necessary to register the different images. Although relative distortions can be handled in software, it's desirable to keep them to a minimum. In the final design, the distortion amounts to 1.0 arcsec between U and Z bands at the edge of the field (Fig. 4).

The design meets the requirements of broad-band imaging, The additional requirement for narrow-band imaging, that any change in effective central wavelength across the field of view be << filter bandwidth (>

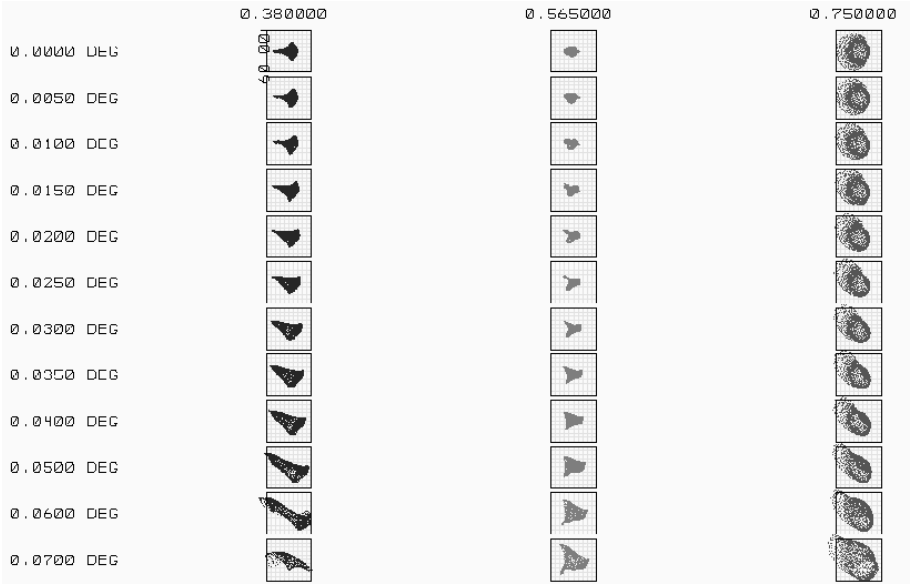

Figure 5. Predicted spot diagram for spectroscopic mode, using a 400 lines mm^{-1} VPH grating in the near-pupil before lens 2 (Fig. 2). The spots are shown for 3 different wavelengths (380, 565, 750 nm, left to right) and as a function of radius in the field (0 – 3.6 arcmin, top to bottom). The box size is 60 microns (1.0 arcsec). The dispersion direction is up-down, in this figure. The implied on-axis spectroscopic resolutions (spot wavelength / spot FWHM, for a 1-arcsec slit) are 290, 430 and 570 for wavelengths 380, 565 and 750 nm respectively. The shape of the spot is determined mainly by optical aberrations due to the disperser not being in a fully-collimated beam. On-axis (radius = 0), the FWHM is much less than 1.0 arcsec, so for this grating, the spectroscopic resolution is limited mainly by the width of the slit.

1.5 nm) is not met. The reason is that the angle of incidence of rays at a filter in the main filter wheels rises approximately linearly with radius in the field, to ≈ 8 deg at radius 4 arcmin. This introduces a wavelength shift ≈ 1.6 nm, which is comparable to the filter bandwidth. The shift rises approximately as the square of the radius, so is considerably less severe at radius 2 arcmin. Nevertheless, the effect would severely vignette imaging of an emission-line galaxy filling the field of view. It is not possible to reduce the wavelength shift significantly without adding more optical surfaces, and this would unacceptably compromise the throughput. A decision was therefore made to allow narrow-band filters to be deployed close to the focal plane, as well as in the main filter wheels. Observers can then decide whether to deploy narrow-band filters in the main filter wheels (suitable for small objects near the centre of the field of view), or near the focal plane (for objects subtending large angular size).

Inclusion of an atmospheric dispersion corrector (ADC) was considered, but rejected at an early stage because of the likely extra cost and complexity, and the loss of throughput. The penalty for not having an ADC is a small elongation of images. This is significant in the blue, e.g. 0.4 arcsec between 400 and 500 nm (a typical blue filter bandpass) at a zenith distance of 30 deg. In the red, the dispersion is negligible.

3.2. Spectroscopy

Given the above design for the imaging, and the desirability of mounting lenses 2 – 6 together in one barrel, the most suitable location for a disperser is in one of the two filter wheels in the near-collimated beam just before lens 2 (Fig. 2). For the required spectroscopic resolution ($R \sim$ few 100), a grism or VPH (volume-phase holographic) grating is required, operating in Littrow configuration (i.e. with no change in the direction of the beam). A grism provides a throughput ≈ 0.5, which is fairly constant with wavelength. A VPH provides a better throughput (≈ 0.8, including the prisms either side) at the blazed wavelength, but the throughput drops off at bluer and redder wavelengths. We expect to purchase at least one VPH and several grisms, to cater for different trade-offs between spectroscopic resolution, wavelength range and throughput. The ruling frequency is

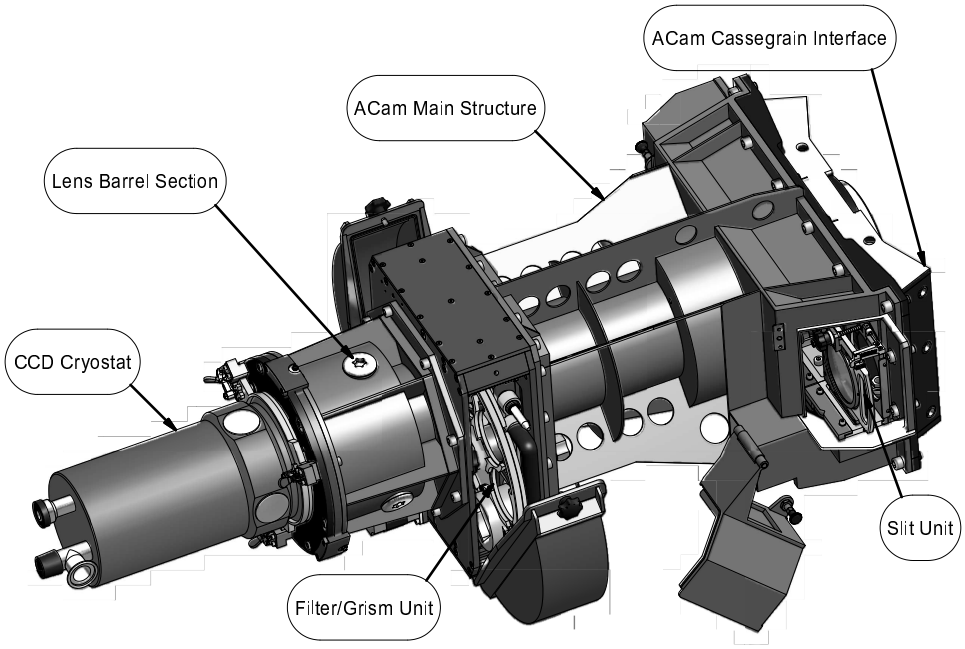

Figure 6. General layout of ACAM, as it will appear when mounted at a folded Cassegrain focus on the side wall of the WHT's Cassegrain A&G box. The total length of the instrument plus cryostat is 1100 mm. ACAM itself (excluding the cryostat) weighs 100 kg.

determined by a combination of the spectroscopic resolution required, and the requirement that the spectrum fit on the CCD. Spot diagrams for a grism with 400 lines mm^{-1} are shown in Fig. 5. With this ruling, the resolution varies from 290 to 570, over the wavelength range 380 to 750 nm (occupying $\approx$ 1100 pixels on the CCD).

Modelling with ZEMAX indicates that no internal focus drive is needed. During commissioning, it will be possible to adjust the position of the slit unit in piston, and this will then be fixed. Residual focus adjustments can be made by changing the telescope focus.

A choice of slits (width 0.5 - 10 arcsec) is provided in the focal plane. The target object will be acquired onto the spectroscopic slit by switching to imaging mode, and acquiring the target on a pre-determined pixel.

Wavelength calibration will be provided by light from the exisiting arc lamps in the Cassegrain A&G unit, relayed to ACAM via a small mirror on a deployable probe.

4. DETECTOR

The detector is a 2k*4k EEV CCD (15-micron pixels) with very low fringing, and readout noise 4 electrons rms, peak QE = 0.9. As noted above, the size of the active area (2k * 2k pixels) is driven by the required field of view (8.3 arcmin) and sampling (0.25 arcsec $pixel^{-1}$). Aditionally, this CCD will act as a spare for other 2k*4k EEV detectors used at the telescope (albeit with the complication that the optically-active cryostat window has to be replaced by a flat window).

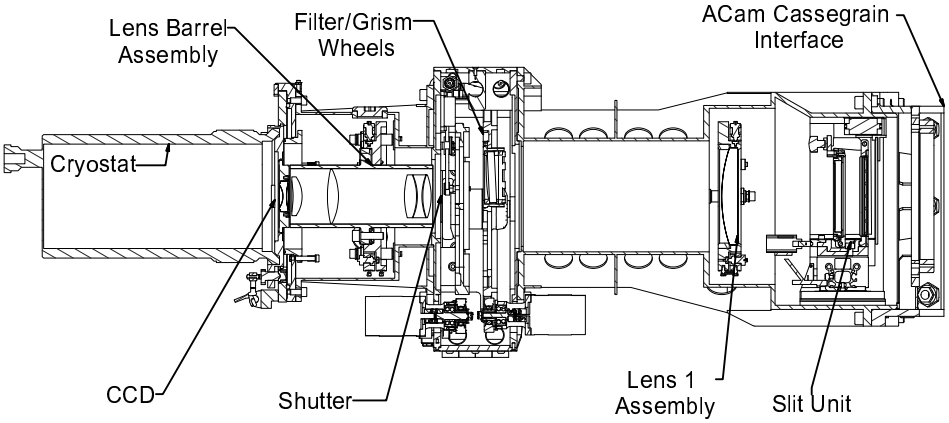

Figure 7. Section view of ACAM.

5. MECHANICAL DESIGN

The mechanical design is driven by the optical design, and by constraints on size, weight and flexure, together with the user requirement that changing filters and grisms in the wheels should be straightforward (and quick). In addition, it's expected that ACAM be integrated into the telescope without modifying existing equipment, and that it be robust, and require minimal maintenance. To achieve this, existing proven technologies are used wherever possible.

The constraints on size, weight and flexure could be alleviated by folding the light path within the instrument, but it was decided at an early stage that this would impose too high a penalty in terms of loss of throughput.

The layout of the final mechanical design is shown in Figs. 6 and 7. It is modular, to allow for removal of the camera when required, and to simplify initial assembly and alignment. The modules are ribbed, for stiffness, and will be dowelled together to allow for repeatable alignment if disassembled. Inspection doors allow access to the slit unit and filter/disperser wheels within a few seconds, without the use of tools.

The main structure is mild steel, rather than aluminium, to minimise thermal expansion. The filter wheels and slit-unit components are aluminium, for ease of manufacture, and for lightness. The number of moving mechanisms has also been kept small (slit-unit carriage, pre-slit mask and 2 filter/grism wheels) to minimise the risk of breakdown. All internal surfaces will be matt black.

The components are described below in light-path order.

5.1. Interface mounting flange

For stiffness, a new mounting flange will be fixed at the current port on the side wall of the Cassegrain A&G box, using the exisiting 230-mm diameter ring of 12 M6 tapped holes, together with two of the strengthening

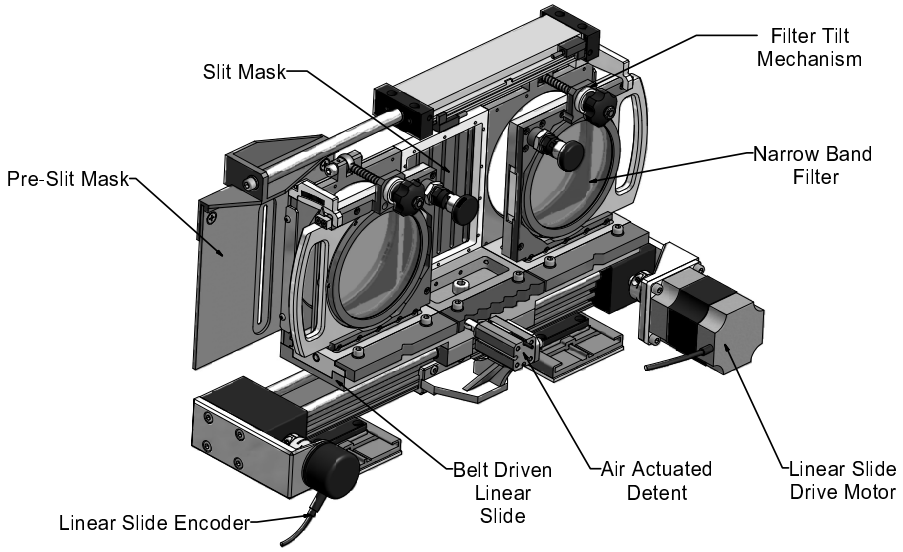

Figure 8. Slit unit, showing the slit mask (mounted on a linear slide), and the pre-slit mask (which allows light to enter only the slit which has been positioned on-axis). The unit also include two mounts for narrow-band filters, with a manual tilt mechanism for fine-tuning the effective central wavelength.

ribs that form part of the Cassegrain box structure.

5.2. Slit unit

Six spectroscopic slits, of different widths (0.5 – 10 arcsec) are cut in a mask mounted on a linear slide (Fig. 8). The slide is moved so as to position the required slit on the optical axis, and a pre-slit mask blocks light from reaching the other slits. The slide has positions for two other masks. One is usually clear (for imaging), the other can be used for a test mask (e.g. pinholes), or in the future might be used for multi-slit masks.

On the back of the slide, there are mounts for two filters, allowing observers the option of mounting narrow-band filters 30 mm behind the focal plane (when it's important to minimise any dependence of central wavelength on radius in the field). These filters can be tilted manually to fine-tune the filter bandpass.

The linear slide is operated by a continuous belt drive, minimising the overall width of the slide for the given range of travel. It is locked in place, accurately and repeatably, by an air-operated detent mechanism. The drive system has been designed with backlash in it to allow the detent mechanism to complete final positioning.

5.3. Lens 1 assembly

The field-lens assembly (Fig. 9) is fully adjustable for alignment (tilt, centring and piston), which relaxes manufacturing tolerances for the main instrument structure.

5.4. Filter / grism wheels

The filter/grism wheels (Fig. 10) are accesible within a few seconds by dropping down a light-tight access cover. Each filter wheel can be independently removed, to replace the filters or grisms, by undoing just one bolt. The wheel's position is defined by guide rails which allow for quick and accurate removal and fitting.

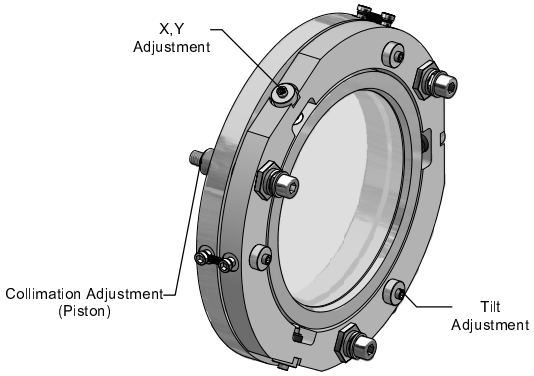

Figure 9. Mount for lens 1 (the field lens), allowing adjustment for centring, piston and tilt.

The filter drive system and the filter detent mechanism are mounted on the back plate. The wheel position is not encoded. Accurate and repeatable positioning is achieved using a friction drive with an active detent mechanism. The detent mechanism comprises a swing arm that activates 2 micro-switches, one for zero-set, one for filter position. When close to the selected position an air-operated detent defines the final position and locks the wheel in place. Zero-setting is achieved by turning the wheel clockwise until the zero-set switch is found, setting the counter, then continuing clockwise, counting how many times the detent filter position switch is activated until it records the home switch again.

Several wheels will be made available to take different combinations of number of filters and filter diameter, e.g. 7 76-mm filters, or 4 125-mm filters.

Filters can be tilted up to 10 deg within the wheels (via counter-rotating rings in the mount), allowing the effective central wavelength of narrow-band filters to be fine-tuned.

The filter box also houses a Prontor shutter, diameter 64 mm. The shutter will be modified for pneumatic control, which is standard for ING instruments. Shutter exposure is controlled by the CCD electronics using existing ING hardware and software.

5.5. Lens barrel

The lens barrel contains lenses 2, 3, 4, 5 and 6. The mounting and adjusting arrangement for the barrel is the same as for Lens 1.

5.6. CCD mounting

A standard ING CCD mounting ring is attached to the lens-barrel support. For initial optical alignment of the crystat (including lens 7, with vacuum seal), it will be possible to move the ring perpendicular to the optical axis, and it will then be fixed in position. The standard mounting ring allows rotation of the cryostat and, via 3 capstans, piston shift and tilt.

5.7. Modifications to the Cassegrain A&G box

Three modifications are required to the A&G box to accommodate the new camera:
(1) The exisiting 45-deg flat will be replaced with a larger (elliptical) flat to intercept the full 8.3-arcmin field.
(2) This flat will be mounted on a turntable, so that any one of 3 folded-Cassegrain ports can be used. This

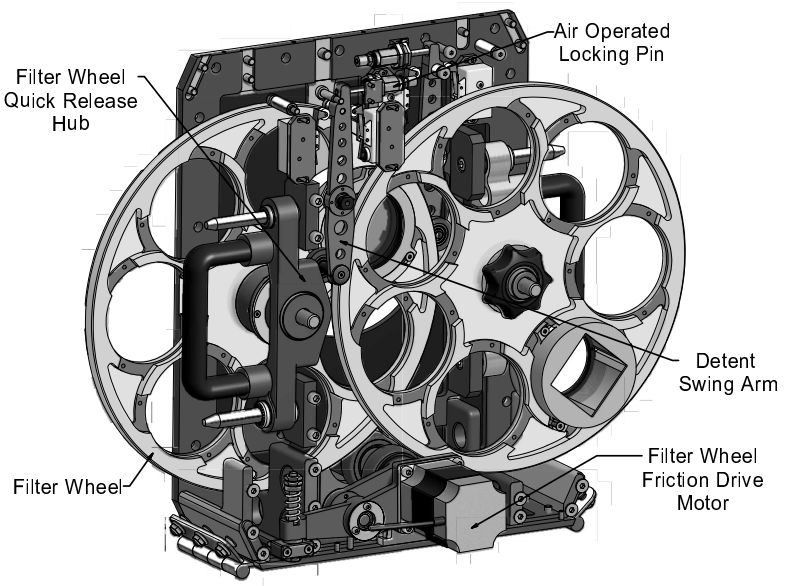

Figure 10. The filter box houses two wheels (for filters and dispersers) and a shutter. The first wheel (leftmost in the figure above) will usually contain a standard set of six broad-band filters (U, B, V, R, I and Z), leaving one position clear. The dipersing element/s will normally be mounted in the second wheel, which is in the pupil plane. The wheels shown here have 7 slots for circular filters of diameter 76 mm. Other wheels will be provided, e.g. with 4 slots of diameter 125 mm.

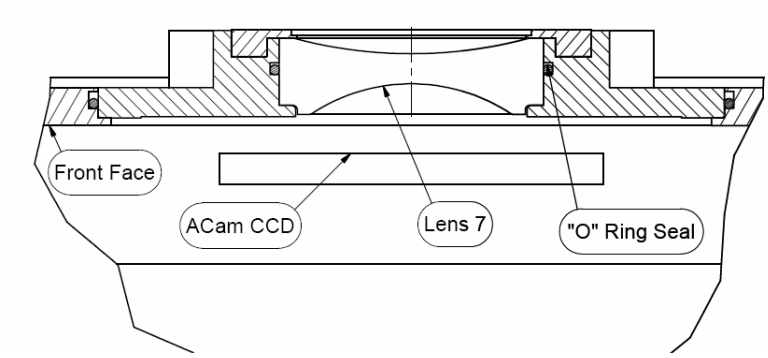

Figure 11. Positioning of lens 7 (the cryostat window) within the front face of the CCD cryostat. Because the window is optically active, the cryostat has to be aligned accurately with the rest of the instrument optics.

adds considerable flexibility, allowing e.g. the WHT's Shack-Hartmann camera to be mounted without removing ACAM.
(3) A small mirror will be mounted on a deployable probe to intercept light from existing calibration lamps (arc lamps) and relay it to ACAM.

No modifications are required to provide autoguiding, which is catered for by the existing Cassegrain autoguider.

6. INSTRUMENT CONTROL

Low-level control will be provided by an Allen Bradley PLC (Programmable Logic Controller). The instrument control hardware and software will be similar to that used recently by ING for another project (a dichroic-filter changer for the WHT's adaptive optics suite), providing considerable savings in programming effort. and on software licences.

The high-level control software for the control server and the user interface will be written in Java and Tcl/Tk respectively.

7. CONCLUSIONS

We have designed a multi-purpose imager/spectrograph, ACAM, to be mounted permanently at the folded Cassegrain focus of the 4.2-m WHT. It will provide seeing-limited broad-band and narrow-band imaging (340 - 1000 nm) over a field of diameter 8.3 arcmin. Low-resolution spectroscopy ($R \sim 500$) will be available at the centre of the field. ACAM can be deployed in ~ 30 sec, less time than it typically takes the WHT to slew to a new target.

It's likely that ACAM will be used for a broad range of high-impact science programmes requiring rapid response (SNe, GRBs), or difficult scheduling (exoplanet transits), or the use of specialised filters (narrow-band H_α imaging of low-redshift galaxies).

The design process involved a trade-off between several demanding science requirements: PSF, field of view, wavelength range, throughput, wavelength shift (for narrow-band imaging) and spectroscopic resolution. An iterative approach was used to ensure that requirements were met in priority order.

The ACAM conceptual design review, and final design review, were held at ING in November 2006 and November 2007 respectively. At the time of writing, the optics and mechanical parts are being manufactured. On-sky commissioning is expected early 2009.

8. ACKNOWLEDGMENTS

Many people have contributed to the development of ACAM over the last two years. These include the ING astronomers who helped frame the science requirements (Romano Corradi, Danny Lennon, Javier Licandro, Rene Rutten, Mischa Schirmer and Ian Skillen) and the ING engineers who work on various aspects of the project (Don Abrams, Craige Bevil, Frank Gribbin, Carlos Martin, Juerg Rey, Simon Tulloch and Michiel van der Hoeven). We're also grateful for advice from Ernesto Sánchez (Fractal), Maria Luisa García (Fractal), Tom Gregory, Johan Knapen (IAC), Chris Pietraszewski (ICOS), Lars Venema (ASTRON) and Sue Worswick (Observatory Optics).

REFERENCES

1. Irwin M., Webster R.L., Hewett P.C., Corrigan R.T., Jedrzejewski R.T., 1989, AJ, 98, 1989
2. Ruiz-Lapuente P. et al, 2004, Nature, 431, 1069
3. Smartt S.J. Maund J.R., Hendry M.A., Tout C.A., Gilmore G.F., Mattila S., Benn C.R., 2004, Science, 303, 499